

# Magnetic field effects on electronic properties of multi-wells quantum rings and dots with an on-center donor impurity

M. SOLAIMANI\*

*Department of Physics, Faculty of science, Qom University of Technology, Qom, Iran*

In this study, we investigate the geometrical potential and magnetic field effects on electronic properties of AlN/GaN Constant Total Effective Radius Multi-Wells Quantum Rings (CTER-MWQRs) and Constant Total Effective Radius Multi-Wells Quantum Dots (CTER-MWQDs) including an on-center donor impurity. We have seen that, the magnetic field effect on ground state energy of single-well CTER-MWQDs is more remarkable than other energy levels. Systems with larger inner quantum rings (or dot) radiuses ( $R_{in}$ ) undertake more changes in ground state energy by increasing the number of wells. We have also shown that for systems with larger  $R_{in}$ , the ground state energy increases more rapidly when the magnetic field increases. For single-well CTER-MWQRs the ground state wave function is localized within the center of the quantum well. At low magnetic fields, maximum probability of finding the electron occurs in the central quantum well while at high magnetic fields the maximum probability occurs at the well which is nearer to the center of the quantum dot (or ring). By increasing the magnetic field, we have stronger localization. The final fact is that, by means of the number of wells, quantum dot (or ring) radiuses and magnetic field, we can control the localization of the ground state wave function (i.e. the free carrier distribution) within our quantum structure and at the same time alter the electronic properties.

(Received November 22, 2017; accepted October 10, 2018)

*Keywords:* Constant total effective radius multi-wells quantum rings, Subband energies, Ground state wave function, Oscillator strength, Magnetic field, On-center donor impurity

## 1. Introduction

During last few years, quantum size effects which are special characteristics of low-dimensional semiconductor quantum structures have been extensively studied both theoretically [1–2] and experimentally [3–4]. Investigations of the impurity states in semiconductor structures are among the crucial problems in semiconductor physics because impurities can dramatically alter the properties and performance of a quantum device.

Besides, experimental fabrication of low dimensional semiconductor hetero-structures has focused great attention on basic physical properties of systems with discrete energy levels. Small ring-shaped semiconductor structures, which have been called quantum rings, can confine electrons in spatial dimensions. Semiconductor quantum rings [5–6] and localized impurity state systems [7–8] are especially intriguing. Through employing the latter systems, we have a unique laboratory to study a single impurity. Fabrication of quantum rings is nowadays possible through lithographic [9], self-assembling [10] and etching [11] techniques. Effects of electric field [12], excitons [13], with Rashba [14] or Dresselhaus [15] spin-orbit coupling and also impurities [16] can produce considerable changes in the electronic properties of the system. By using these parameters, one is able to control or modulate the intensity outputs of optoelectronic devices.

Thus, here we have selected this target system for our study.

In our previous studies we have investigated the electronic properties of three-electron-quantum dot under the influence of the Rashba coupling [17], electronic properties of spinless particles subjected to the Yukawa potential [18], D-dimensional Schrödinger equation with Woods-Saxon potential, spin-orbit, coulomb and centrifugal terms through a new hybrid numerical fitting Nikiforov-Uvarov method [19], repetitive states in one dimensional Hubbard model by density matrix renormalization group method [20], electronic and optical properties [12–21] of constant total effective length multiple quantum well systems and also donor impurity effects on electronic and optical properties of GaN/AlN constant total effective radius multi-shell spherical quantum dots [22]. In the current work, we have studied the effect of the number of wells, inner and outer quantum ring radiuses as well as cylindrical dot radius and magnetic field on the electronic properties of GaN/AlN constant total effective radius multi-wells quantum rings (CTER-MWQRs).

## 2. Formalism

Radial part of the Schrödinger equation in the cylindrical coordinates (through separation of variables

technique) within the envelope-function approximation via effective mass technique for a quantum ring (or cylindrical quantum dot) with an on-center donor impurity under the influence of a uniform magnetic field  $B$  along the  $z$  direction can be written as [23-25]:

$$-\frac{\hbar^2}{2} \frac{\partial}{\partial \rho} \left( \frac{1}{m^*} \frac{\partial R_{n,l}}{\partial \rho} \right) - \frac{\hbar^2}{2m^*} \frac{1}{\rho} \frac{\partial R_{n,l}}{\partial \rho} + \frac{\hbar^2}{2m^*} \frac{m^2}{\rho^2} R_{n,l} + \frac{1}{2} m \hbar \omega_c + \frac{1}{8} m^* \omega_c^2 \rho^2 + V(\rho) R_{n,l} - \frac{e^2}{4\pi\epsilon\epsilon_0 r} = ER_{n,l} \quad (1)$$

where  $m^*$  is the effective mass,  $m = 0, \pm 1, \pm 2, \dots$  is magnetic quantum number and  $\omega_c = eB/m^*$  is the cyclotron frequency. We have also defined the geometrical confining potential  $V(\rho)$  as:

$$V(\rho) = \begin{cases} V_{conf} & i = 1, 3, \dots; \frac{i-1}{2N+1} R_{in} < \rho < \frac{i}{2N+1} R_{out} \\ 0 & i = 2, 4, \dots \end{cases} \quad (2)$$

Here,  $N$  is the number of wells,  $l$  is the orbital quantum number,  $V_{conf}$  in the constant relative conduction band offset and  $i$  shows the  $i$ 'th well or barrier.  $R_{in}$  and  $R_{out}$  are inner and outer quantum dot shell radiuses respectively. The eigen-energies and eigen-function have been calculated through numerical discretization techniques [26]. The boundary condition has been applied in the numerical procedure. However, since its description, applying boundary condition and etc. is available elsewhere [27-30], we have not described it in our manuscript, again.

Oscillator strength is an important parameter because it governs the probability distributions and optical properties of the systems. Oscillator strength can be defined as,

$$O_{fi} = \frac{2m^*}{3\hbar^2} (E_{n,l}^f - E_{n,l}^i) \left| \int R_{n,l}^f | \rho^3 | R_{n,l}^i d\rho \right|^2 \quad (3)$$

Transition probabilities can be determined by oscillator strength. The summation over oscillator strengths due to all possible transitions between states is 1. This fact can analytically be written as,

$$\sum_f O_{fi} = 1 \quad (4)$$

### 3. Results and discussion

In our calculations, we have taken  $m = 0.15m_0$  (where  $m_0$  is the free electron mass), the barrier height  $V_{conf} = 1.28$  eV, the different inner (0, 200, 400 and 600  $\text{\AA}$ ) and outer (400, 600 and 1000  $\text{\AA}$ ) quantum ring radiuses. Then, we have obtained the ground state energies, wavfunctions and oscillator strengths for different number of wells, ring

inner and outer quantum ring radiuses through numerical solution of the equation (1). We have also studied the effect of the magnetic field on the abovementioned electronic properties.

In QDs, the selection rules ( $\Delta l = \pm 1$ ) determine the final state of the exciton after the absorption. Hence, we restrict our study to the transition of the ground state ( $l = 0, m=0$ ) to the first excited state ( $l = 1, m=1$ ).

In panels of the Fig. 1, we have shown the ground state energy as a function of the magnetic field for CTER-MWQRs with different numbers of wells. In both panels, we have assumed outer quantum ring radius  $R_{out}=400\text{\AA}$ . However, in the panel (A), inner quantum ring radius is  $R_{in}=0\text{\AA}$  and in the panel (B),  $R_{in}=200\text{\AA}$ . As we can see in the panel (A) of this figure, the effect of the magnetic field on ground state energy of single-well CTER-MWQDs is more remarkable. It seems that the ground state energy of CTER-MWQDs with more number of wells do not change too much when the magnetic field increases. However, when we increase the magnetic field, the ground state energy do not change too much for  $R_{in}=0\text{\AA}$  and increase slowly for  $R_{in}=200\text{\AA}$ . In this panel, we see that by increasing of the number of wells, the ground state energy increases. This can be expected, since when we fix the quantum dot radius and increase the number of well inside it, gradually the well widths decrease. However, as we know from the quantum mechanics, narrower quantum wells have larger ground state energies (e.g. for infinite single quantum well: energy levels are:  $E_n = n^2 \pi^2 \hbar^2 / 2mL^2$ , where  $L$  is the well width).

Now, we increase the inner quantum dot radius  $R_{in}=200\text{\AA}$ . Now, the variation of the ground state energy as a function of the magnetic field can be found in the panel (B). Here, we have some differences with the panel (A). We see that, systems with larger  $R_{in}(=200\text{\AA})$  are more sensitive to magnetic field (i.e. the ground state energy changes more). Another fact is that, in systems with larger  $R_{in}$ , increasing of the number of wells changes the ground state energy more. In panel (A) increasing of the number of well to 10 leads to increasing of the ground state energy to 300meV but in the panel (B), only increasing of the number of well to 5 leads to increasing of the ground state energy to around 300 meV. We have not increased the number of wells more, because more increasing of the number of wells leads to very thin quantum wells which its experimental fabrication is difficult. Because, if we create six wells in between  $R_{in}=200\text{\AA}$  and  $R_{out}=400\text{\AA}$ , based on the equation (2) we will have 7 number of barriers. Therefore, since we have assumed same well and barrier length, the length of each barriers and wells is  $200/(6+7)\text{\AA} \approx 15\text{\AA}$ .

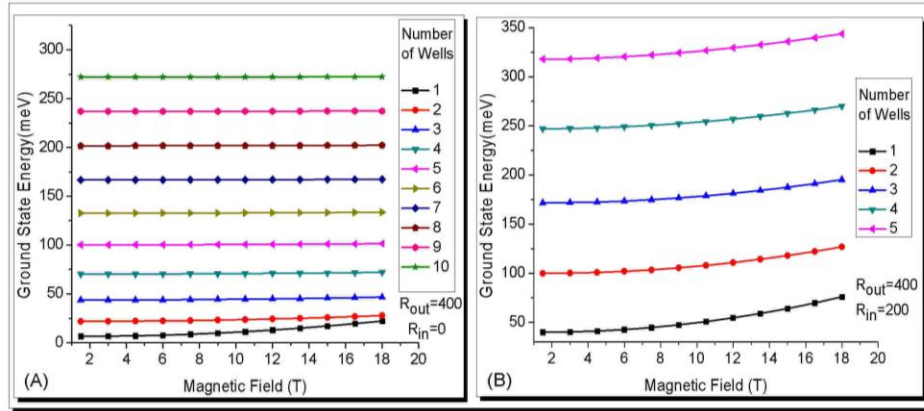


Fig. 1. Ground state energy as a function of the magnetic field for CTER-MWQRs with different numbers of wells (1 to 10). In both panels, we have assumed  $R_{out}=400A^0$  while in panel (A),  $R_{in} = 0A^0$  and in the panel (B),  $R_{in}=200A^0$

Now, we have repeated the Fig. 1 but here, we have assumed  $R_{out}=600A^0$ . Within the Fig. 2, in panel (A), we set  $R_{in}=0A^0$  and numbers of wells (1 to 10), in the panel (B),  $R_{in}=200A^0$  and numbers of wells (1 to 10) and also in the panel (C),  $R_{in}=400A^0$  and numbers of wells (1 to 5). All facts we have mentioned above about the Fig. 1, are true about this figure too but there are some additional facts here. At this figure, by increasing of the magnetic field, the ground state energy of the CTER-MWQDs with one number of wells can grow with more speed than CTER-MWQDs with more number of wells. This can be seen through level crossing point in this figure. However by increasing of the inner quantum dot radius  $R_1$ , this level

crossing can be removed (see panel (C) of the Fig. 2). Finally, we have to note that, for systems with larger  $R_{in}$ , when we increase the magnetic field the ground state energy increases more rapidly. In order to show the effects of the magnetic field, quantum ring and dot thicknesses and number of wells on the ground state energy we have presented the Fig. 3 which is similar to Fig. 1. Here, we have assumed the numbers of wells (1 to 10) and  $R_{out}=1000A^0$ . In panel (A), we set  $R_{in}=0A^0$ , in the panel (B),  $R_{in}=200A^0$ , in the panel (C),  $R_{in}=400A^0$  and also in the panel (D),  $R_{in}=600A^0$ .

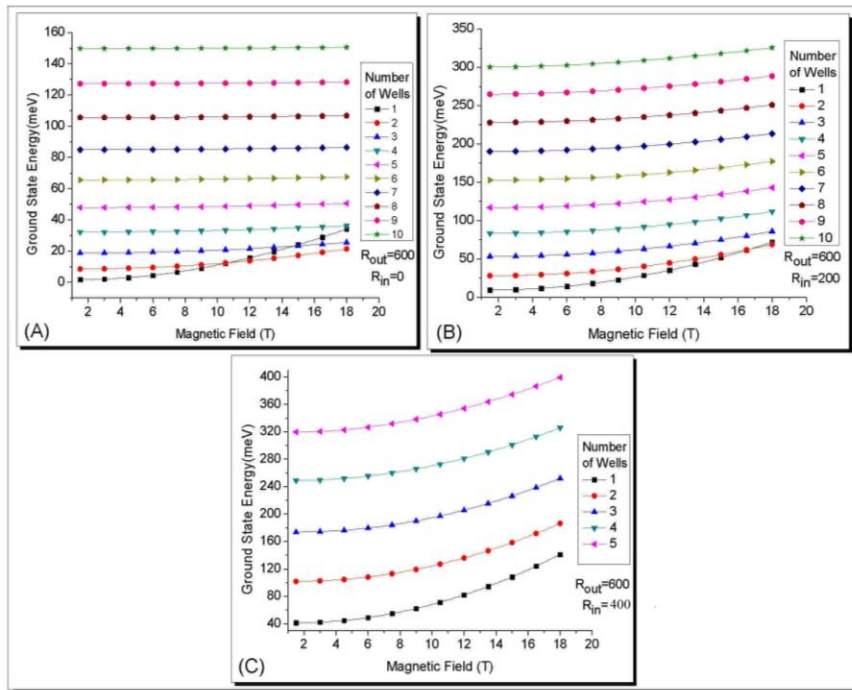


Fig. 2. Same as Fig. 1 but here, we have assumed  $R_{out}=600A^0$ . In panel (A), we set  $R_{in}=0A^0$  and numbers of wells (1 to 10), in the panel (B),  $R_{in}=200A^0$  and numbers of wells (1 to 10) and also in the panel (C),  $R_{in}=400A^0$  and numbers of wells (1 to 5)

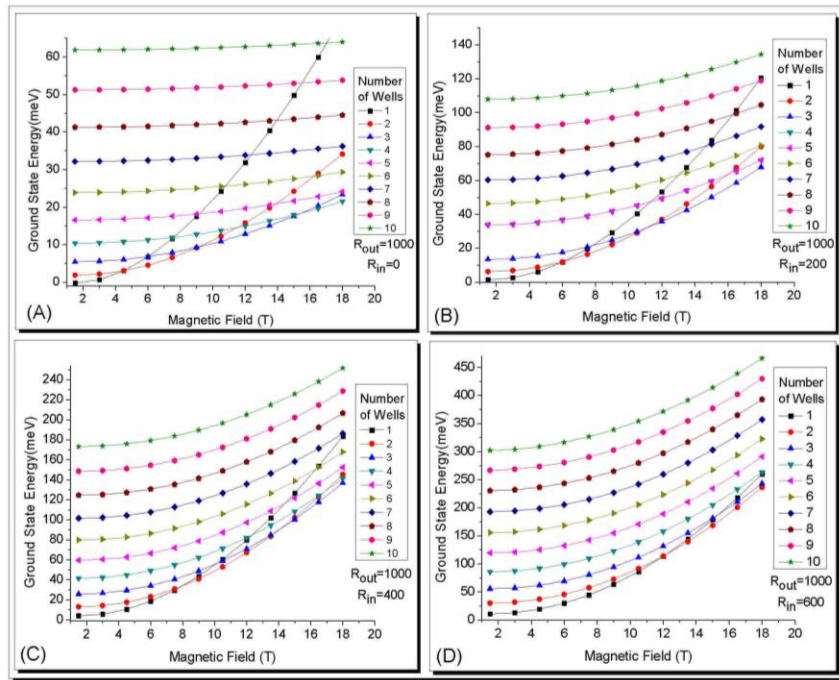


Fig. 3. Same as Fig. 1 but here, we have assumed the numbers of wells (1 to 10) and  $R_{out}=1000A^0$ . In panel (A), we set  $R_{in}=0 A^0$ , in the panel (B),  $R_{in}=200 A^0$ , in the panel (C),  $R_{in}=400 A^0$  and also in the panel (D),  $R_{in}=600 A^0$

At this point we study the ground state normalized wave function for CTER-MWQRs when  $R_{out}=400A^0$ . We have plotted it as a function of the magnetic field (T, i.e. Tesla) and position ( $A^0$ , i.e. angstrom) in the Fig. 4. Number of wells and  $R_{in}$  in panels (A) to (D) are ( $0 A^0$  & 1), ( $0 A^0$  & 4), ( $200 A^0$  & 1) and ( $200 A^0$  & 4), respectively. As it is clear, for single-well CTER-MWQRs with  $R_{in}=0 A^0$  and  $R_{in}=200 A^0$  the ground state wave function is localized within the center of the quantum well. If we increased the number of wells to four the situation changes. If we select  $R_{in}$  to be  $0 A^0$ , the wave function is strongly and completely localized within the quantum well which is the nearest one to the center of the quantum ring (or dot). However, if we increase the inner quantum dot (or ring) to  $R_{in}=200 A^0$ , this strong localization of the wave function will be destroyed. Here, the probability of finding the electron within the other quantum wells is not zero anymore. The probability of finding the electron decreases along the radius (i.e. the height of the wave function peaks decreases along the radius. Since the wave function peaks are located in the quantum wells, thus the peak heights of the wave function which their corresponding quantum wells placed at farther regions of the radius are smaller). In the panels (A) to (C) the effect of the magnetic field is not so remarkable. But in the panel (D), we can see that at low magnetic fields, maximum probability of finding the electron have been taken place in the central quantum well while at high magnetic fields the maximum probability occurs at the well which is nearer to the center of the quantum dot (ring). Thus by means of the

number of wells, quantum dot (or ring) thickness and magnetic field we can control the localization of the ground state wave function and hence control the free carrier distribution within our quantum structure. In order to show the effects of the magnetic field, quantum ring and dot thicknesses and number of wells more visibly, we have presented the Fig. 5, which is same as Fig. 4 but here for  $R_{out}=600A^0$ . Number of wells and  $R_{in}$  in panels (A) to (F) are ( $0 A^0$  & 1), ( $0 A^0$  & 4), ( $200 A^0$  & 1), ( $200 A^0$  & 4), ( $400 A^0$  & 1) and ( $400 A^0$  & 4), respectively. As a consequence, we think this scenario should go on for larger  $R_{out}=1000A^0$  but this is not true. In the Fig. 6, we have repeated the Fig. 5 but here for  $R_{out}=1000A^0$ . Number of wells and  $R_{in}$  in panels (A) to (H) are ( $0 A^0$  & 1), ( $0 A^0$  & 4), ( $200 A^0$  & 1), ( $200 A^0$  & 4), ( $400 A^0$  & 1) and ( $400 A^0$  & 4), ( $600 A^0$  & 1) and ( $600 A^0$  & 4), respectively. If we see the panel (A) of this figure we see that, by increasing of the magnetic field the amplitude of the ground state wave function increases by increasing of the magnetic field and at the same time the full width at half maximum (FWHM) of the ground state decreases (stronger localization). Due to the free charge carrier conservation, we had expected this fact to be occurred. Another difference with Figs. 4 and 5 is that, by increasing of the inner quantum dot (or ring) radius  $R_{in}$  or number of wells the localization will not be destroyed. For these systems (different panels of the Fig. 6) the probability of finding the electron in only one quantum well is not zero.

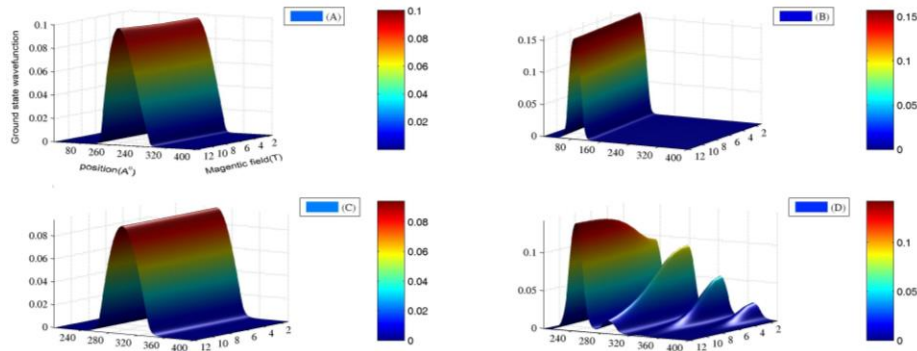


Fig. 4. Ground state normalized wave function for CTER-MWQRs with  $R_{out}=400A^0$  as a function of the magnetic field ( $T$ ) and position ( $A^0$ ). Number of wells and  $R_{in}$  in panels (A) to (D) are  $(0 A^0 \& 1)$ ,  $(0 A^0 \& 4)$ ,  $(200 A^0 \& 1)$  and  $(200 A^0 \& 4)$ , respectively

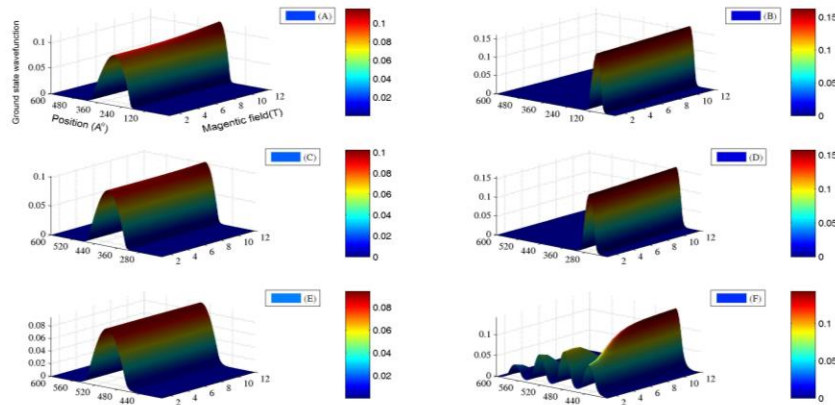


Fig. 5. Same as Fig. 4 but here for  $R_{out}=600A^0$ . Number of wells and  $R_{in}$  in panels (A) to (F) are  $(0 A^0 \& 1)$ ,  $(0 A^0 \& 4)$ ,  $(200 A^0 \& 1)$ ,  $(200 A^0 \& 4)$ ,  $(400 A^0 \& 1)$  and  $(400 A^0 \& 4)$ , respectively

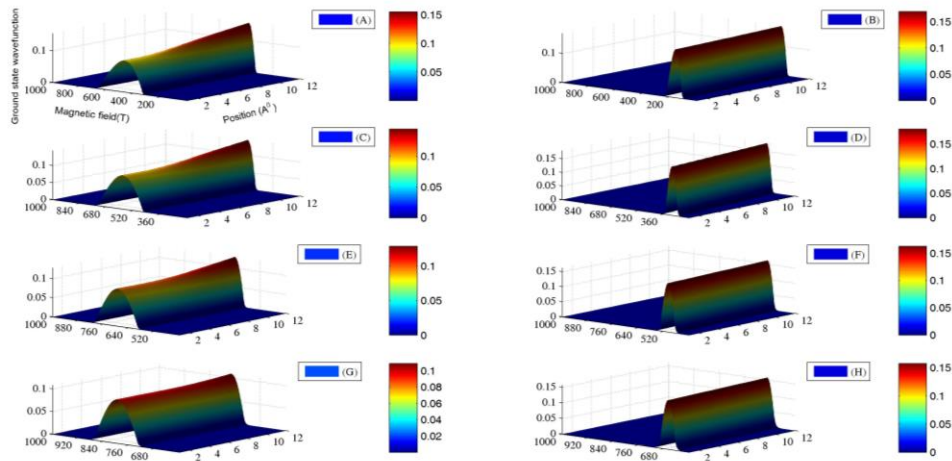


Fig. 6. Same as Fig. 4 but here for  $R_{out}=1000A^0$ . Number of wells and  $R_{in}$  in panels (A) to (H) are  $(0 A^0 \& 1)$ ,  $(0 A^0 \& 4)$ ,  $(200 A^0 \& 1)$ ,  $(200 A^0 \& 4)$ ,  $(400 A^0 \& 1)$  and  $(400 A^0 \& 4)$ ,  $(600 A^0 \& 1)$  and  $(600 A^0 \& 4)$ , respectively

The probability of emission or absorption of electromagnetic radiation in transitions between subband energy levels within a spectroscopy can be described through oscillator strength (a dimensionless quantity). We have calculated this quantity for our quantum structures. Fig. 7 shows the variation of the oscillator strength as a

function of the magnetic field for CTER-MWQRs with different numbers of wells (1 to 7). In both panels, we have assumed  $R_{out}=400A^0$  while in panel (A),  $R_{in}=0 A^0$  and in the panel (B),  $R_{in}=200 A^0$ . In the panel (A), we see that the effect of the magnetic field on the oscillator strength is not too much. However when we increase the

number of wells the oscillator strength decreases. In the panel (B) with larger  $R_{in}(=200 \text{ \AA}^0)$ , effect of the magnetic fields on oscillator strength is small for systems with few number of wells while its effect on systems with larger number of wells is large. In the meantime, for systems with larger number of wells, the oscillator strength increases when the magnetic field increases. Now, we increase the  $R_{out}$  to  $600 \text{ \AA}^0$  to obtain the Fig. 8. It is same as Fig. 7 but here, we have assumed  $R_{in}=0 \text{ \AA}^0$  and numbers of wells (1 to 7) in panel (A),  $R_{in}=200 \text{ \AA}^0$  and numbers of wells (1 to 7) in the panel (B), and  $R_{in}=400 \text{ \AA}^0$  and numbers of wells (1 to 5) in the panel (C). Just as we had seen in the Fig. 7, the effect of the magnetic field on the oscillator strength is small for  $R_{in}=0 \text{ \AA}^0$  in panel (A). In the panels (B) and (C) with larger  $R_{in}(=200 \text{ \AA}^0$  and  $400 \text{ \AA}^0)$ , effect of the magnetic fields on oscillator strengths are

small for systems with few number of wells while its effect on systems with larger number of wells is large. This fact is exactly the same as what was true for  $R_{out}=400 \text{ \AA}^0$  in the Fig. 7. This means, changing the  $R_{out}$  does not affect on the behavior of the oscillator strength under the influence of the magnetic field, number of wells and inner quantum dot radius  $R_{in}$ . In order to show the effects of the magnetic field, quantum ring and dot thicknesses and number of wells on the oscillator strength we have presented the Fig. 9 which is same as Fig. 8 but here, we have assumed the numbers of wells (1 to 7) and  $R_{out}=1000 \text{ \AA}^0$ . In panel (A), we set  $R_{in}=0 \text{ \AA}^0$ , in the panel (B),  $R_{in}=200 \text{ \AA}^0$ , in the panel (C),  $R_{in}=400 \text{ \AA}^0$  and also in the panel (D),  $R_{in}=600 \text{ \AA}^0$ .

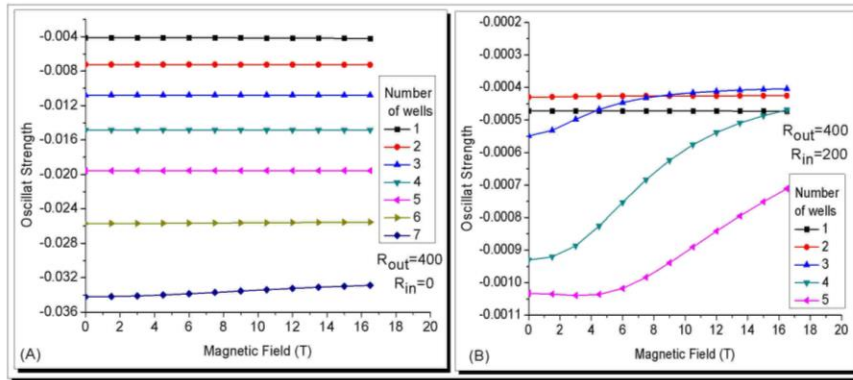


Fig. 7. Variation of the oscillator strength as a function of the magnetic field for CTER-MWQRs with different numbers of wells (1 to 7). In both panels, we have assumed  $R_{out}=400 \text{ \AA}^0$  while in panel (A),  $R_{in}=0 \text{ \AA}^0$  and in the panel (B),  $R_{in}=200 \text{ \AA}^0$

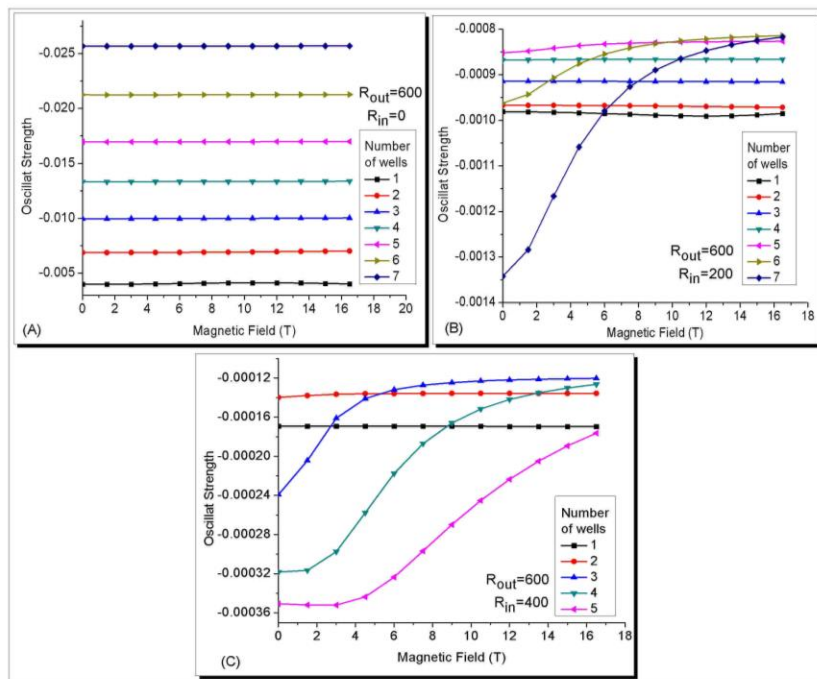


Fig. 8. Same as Fig. 7 but here, we have assumed  $R_{out}=600 \text{ \AA}^0$ . In panel (A), we set  $R_{in}=0 \text{ \AA}^0$  and numbers of wells (1 to 7), in the panel (B),  $R_{in}=200 \text{ \AA}^0$  and numbers of wells (1 to 7) and also in the panel (C),  $R_{in}=400 \text{ \AA}^0$  and numbers of wells (1 to 5)

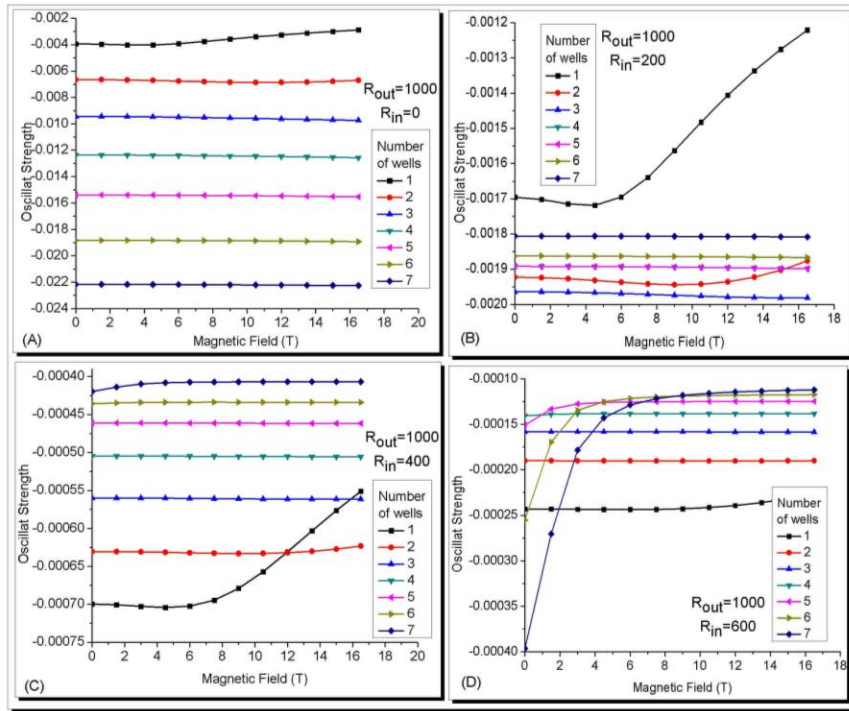


Fig. 9. Same as figure (8) but here, we have assumed the numbers of wells (1 to 7) and  $R_{out}=1000A^0$ . In panel (A), we set  $R_{in}=0A^0$ , in the panel (B),  $R_{in}=200A^0$ , in the panel (C),  $R_{in}=400A^0$  and also in the panel (D),  $R_{in}=600A^0$

#### 4. Conclusion

In this work, we studied the effect of the magnetic field, number of wells and quantum ring and dot thicknesses on electronic properties of AlN/GaN constant total effective radius multi-wells quantum rings and dots. We showed that, the effect of the magnetic field on ground state energy of single-well CTER-MWQDs is more remarkable than other energy levels. By increasing of the number of wells, the ground state energy increased. In systems with larger  $R_{in}$ , increasing of the number of wells changed the ground state energy more. For systems with larger  $R_{in}$ , when we increased the magnetic field the ground state energy increased more rapidly. For single-well CTER-MWQRs the ground state wave function was localized within the center of the quantum well. At low magnetic fields, maximum probability of finding the electron took place in the central quantum well while at high magnetic fields the maximum probability occurs at the well which was nearer to the center of the quantum dot (or ring). By increasing of the magnetic field we had stronger localization. Effects of the number of well, quantum ring and dot radiuses and magnetic fields on oscillat strength was somewhat complicated which we described in the text completely. Thus by means of the number of wells, quantum dot (or ring) thickness and magnetic field we could control the localization of the ground state wave function and hence control the free carrier distribution within our quantum structure.

#### Acknowledgment

We are grateful for Qom University of Technology supports.

#### References

- [1] F. A. P. Osorio, M. H. Degani, O. Hipolito, Phys. Rev. B **37**, 1402 (1988).
- [2] Y. Wu, L. M. Falicov, Phys. Rev. B **29**, 3671 (1984).
- [3] P. Ramvall, S. Tanaka, S. Nomura, P. Riblet, Y. Aoyagi, Appl. Phys. Lett. **73**, 1104 (1998).
- [4] J. A. Yater, K. Kash, W. K. Chan, T. S. Ravi, T. J. Gmitter, L. T. Florez, J. P. Harbison, Appl. Phys. Lett. **65**, 460 (1994).
- [5] R. Blossey, A. Lorke, Phys. Rev. E **65**, 021603 (2002).
- [6] D. Granados, J. M. Garcia, Appl. Phys. Lett. **82**, 2401 (2003).
- [7] J. W. Sakai, P. C. Main, P. H. Beton, N. La Scala Jr., A. K. Geim, L. Eaves, M. Henini, Appl. Phys. Lett. **64**, 2563 (1994).
- [8] J. W. Sakai, N. La Scala Jr, P. C. Main, P. H. Beton, T. J. Foster, A. K. Geim, L. Eaves, M. Henini, G. Hill, M. A. Pate, Solid-State Electron. **37**, 965 (1994).
- [9] M. Bayer, O. Stern, P. Hawrylak, S. Safard, A. Forchel, Nature (London) **405**, 923 (2000).
- [10] M. D. Teodoro, V. L. Campo, V. Lopez-Richard, E. Marega, G. E. Marques, Y. G. A. Gobato, F. Iikawa, M. J. S. P. Brasil, Z. Y. Abu Waar, V. G. Dorogan, Y. I. Mazur, M. Benamara, G. J. Salamo, Phys. Rev. Lett.

- 104**, 086401 (2010).
- [11] F. Ding, N. Akopian, B. Li, U. Perinetti, A. Govorov, F. M. Peeters, C. C. Bof Bufon, C. Deneke, Y. H. Chen, A. Rastelli, O. G. Schmidt, V. Zwiller, *Phys. Rev. B* **82**, 075309 (2010).
- [12] M. Solaimani, M. Izadifard, H. Arabshahi, M. R. Sarkardei, *Journal of Lumin.* **134**, 699 (2013).
- [13] A. O. Govorov, A.V. Kalameitsev, R. Warburton, K. Karrai, S. E. Ulloa, *Physica E* **13**, 297 (2002).
- [14] J. Splettstoesser, M. E. Governale, U. Zulicke, *Phys. Rev. B* **68**, 165341 (2003).
- [15] M. Nita, D. C. Marinescu, A. Manolescu, B. Ostahie, V. Gudmundsson, *Physica E* **46**, 12 (2012).
- [16] H. M. Baghramyan, M. G. Barseghyan, A. A. Kirakosyan, R. L. Restrepo, M. E. Mora-Ramos, C. A. Duque, *J. Lumin.* **676**, 145 (2014).
- [17] H. Hassanabadi, M. Solaimani, H. Rahimov, *Solid State Commun.* **151**, 1962 (2011).
- [18] M. Hamzavi, S. M. Ikhdaier, M. Solaimani, *Int. J. Mod. Phys. E* **21**, 1250016 (2012).
- [19] A. Niknam, A. A. Rajabi, M. Solaimani, *J. Theor. Appl. Phys.*, DOI 10.1007/s40094-015-0201-9.
- [20] M. Solaimani, *J. Nano-and- Electronic Phys.* **7**, 04101(2015).
- [21] M. Solaimani, M. Izadifard, H. Arabshahi, M. R. Sarkardei, *Journal of Lumin.* **134**, 88 (2013).
- [22] M. Solaimani, M. Ghalandari, L. Lavaei, *J. Opt. Soc. America B* **33**, 421 (2016).
- [23] M. Amado, R. P. A. Lima, C. González-Santander, F. Domínguez-Adame, *Phys. Rev. B* **76**, 073312 (2007).
- [24] V. Arsoski, M. Tadic, F. M. Peeters, *Acta Physica Polonica A*, **117**, 733 (2010).
- [25] B. Boyacioglu, A. Chatterjee, *Physica B* **407**, 3535 (2012).
- [26] William H. Press, Saul A. Teukolsky, William T. Vetterling, Brian P. Flanner, *Numerical Recipe, Third Edition*, Cambridge University Press (2007).
- [27] M. Amado, R. P. A. Lima, C. González-Santander, F. Domínguez-Adame, *Phys. Rev. B* **76**, 073312 (2007).
- [28] T. Ando, Y. Ohtake, N. Ohtani, *Phys. Rev. E* **73**, 066702 (2006).
- [29] Yoshimasa Murayama, *Mesoscopic Systems: Fundamentals and Applications*, Wiley-VCH Verlag, Berlin Ornhi, 2001.
- [30] J. D. Cooper, A. Valavanis, Z. Ikonc, P. Harrison, J. E. Cunningham, *J. Appl. Phys.* **108**, 113109 (2010).

---

\*Corresponding author: solaimani@qut.ac.ir;  
solaimani.mehdi@gmail.com